Advanced imaging and spectroscopy techniques for body magnetic resonance

Heer, P. de

2

INCREASING SIGNAL HOMOGENEITY AND IMAGE QUALITY IN ABDOMINAL IMAGING AT 3 T WITH VERY HIGH PERMITTIVITY MATERIALS

2 INCREASING SIGNAL HOMOGENEITY AND IMAGE QUALITY IN ABDOMINAL IMAGING AT 3 T WITH VERY HIGH PERMITTIVITY MATERIALS

Adapted from Magnetic Resonance in Medicine 2012 Oct;68(4):1317-2.

Authors
P. de Heer,[1,2] W. M. Brink,[2] B. J. Kooij,[1] and A. G. Webb[2*]

[1] Department of Telecommunications, Technical University of Delft, Delft, The Netherlands.

[2] C.J. Gorter Center for High Field MRI, Department of Radiology, Leiden University Medical Center, Leiden, The Netherlands.

ABSTRACT
The appearance of severe signal drop-outs in abdominal imaging at 3 T arises primarily from areas of very low B_1^+ transmit field in the body, and is problematic in both obese as well as very thin subjects. In this study, we show how thin patient-friendly pads containing new high permittivity materials can be designed and optimized, and when placed around the subject increase substantially the B_1^+ uniformity and the image quality. Results from nine healthy volunteers show that inclusion of these dielectric pads results in statistically significant decreases in the coefficient of variance of the B_1^+ field, with stronger and more uniform fields being produced. In addition there are statistically significant decreases in timeaveraged power required for scanning. These differences are present in both quadrature-mode operation (coefficient of variance decrease, $P < 0.0001$, mean 25.4 ± 10%: power decrease, $P = 0.005$, mean 14 ± 14%) and also for the RF shimmed case (coefficient of variance decrease, $P = 0.01$, mean 16 ± 13%: power decrease, $P = 0.005$, mean 22 ± 11%) of a dual-transmit system.

INTRODUCTION
The appearance of signal voids in abdominal MRI in both volunteers and patients at 3 T has been noted by many researchers.[1–6] Some report that severely obese patients present the worst situation,[2] others that this effect also occurs for very thin patients.[1,3] As noted by Bernstein [1] ''Image shading and uneven contrast resulting from spatial variation in the transmit B_1^+ field remains one of the biggest unsolved problems for routine clinical 3 T imaging today.'' The phenomenon of signal loss is often referred to as ''dielectric resonance.'' Pregnant women and patients with ascites are universally problematic, and subsequently are almost always studied at 1.5 T.[5,6] The clinical, and implicitly financial, importance of this situation is emphasized by the recent commercial introduction of dual-transmit RF systems at 3 T, in which the quadrature body coil is effectively split into two linear coils, each of which can be driven with an independently controlled magnitude and phase. The two degrees of freedom (relative amplitudes and relative phases of the two channels) compared to only one (absolute amplitude) for a conventional single transmit system can produce considerable increases in RF transmit homogeneity,[7,8] as has long been known theoretically and investigated extensively for imaging at 7 T.[9–11] However, experience at our institution and elsewhere indicates that, despite improved performance, dual-channel 3 T systems do not consistently solve the problem of image inhomogeneities. Experimental and simulation work has suggested that there are still further improvements using an eight channel transmit body coil,[12,13] but such a setup is not currently commercially available.

A second approach to address the issues of RF inhomogeneity in 3 T abdominal imaging is the use of ''dielectric pads''.[14–17] Previous very simple pads typically are made from ultrasound gel with dissolved paramagnetics such as manganese chloride to give a short T^2 and hence low background MR signal. Some institutions report that these are used locally for most abdominal scans,[15] whereas others report that they are not commonly used in the wider community.[1] There are several problems with this approach as currently implemented. From a practical point-of-view the pad is 3 cm thick and therefore somewhat patient-unfriendly. In the usual implementation, a single pad is placed centrally on top of the patient irrespective of the patient size: the large thickness makes it impractical to place a second one underneath the patient to improve the transmit field in the posterior regions. Perhaps most importantly, no optimization of the properties (size, shape, thickness, placement, or relative permittivity) of the dielectric pad or material has been shown.

In this article, we present both electromagnetic (EM) simulations and experimental data using thin pads with high permittivity materials based upon aqueous suspensions of metal titanates which have a relative permittivity of 300.[18,19] Placement of two of these thin (1 cm) pads anterior and posterior to the subject is shown to improve significantly both the transmit field homogeneity and the overall image quality. The imaging performance both with and without dielectric pads is compared experimentally to that of a dual-channel RF system in quadrature mode, as well as the combined approach using both the dielectric pads and RF shimming. Significant improvements in homogeneity due to the pads are found when the scanner is used in the conventional quadrature mode, and the best performance is found using RF shimming combined with the high permittivity pads.

METHODS

EM Simulations

A commercial package based on a finite difference time domain method (xFDTD, Remcom, PA) was used for all simulations. The RF coil was modeled as a 16 rung high pass birdcage coil with a diameter of 61 cm, length 56 cm, driven in quadrature mode by 32 ideal current sources with an impedance of 50 V. This corresponds to a dual transmit system being operated in the conventional quadrature or fixed phase mode, in which the phase relationship between the two channels is fixed at 90°. One male (Duke, body mass index 23) or one female (Ella, body mass index 22) model from the virtual family was placed in the center of the coil.[20] An isotropic grid cell size of 2.5 mm was used with a seven-layer perfectly matched absorbing boundary. A sinusoidal current was applied at 128 MHz, with a timestep of 4.8 ps. A criterion of -50 dB was set for convergence of the steady-state fields, and typical simulation times were 30 min using a graphics processing unit. The transmit magnetic field (B_1^+), electric (E) field, and specific absorption rate (SAR) were simulated for each configuration: normalization was to 1 W dissipated power.

To determine the optimal pad permittivity, a grid search was used in which the relative permittivity values of two pads (one anterior, one posterior), each of thickness 1 cm, were varied from 1 to 650 in steps of 50. For comparison, a 3 cm thick commercially available water pad was included in the simulations.[14,15] The coefficient of variation (C_v) of the B_1^+ field, i.e., 100 multiplied by the standard deviation of the B_1^+ divided by its mean value, across the simulated B_1^+ map (transverse orientation) was evaluated in MATLAB (Mathworks, Natick, MA). In the transverse slices, the value of C_v is calculated throughout the entire cross-section (not considering the arms). For coronal slices, a rectangular region of interest is assigned through the thorax and abdominal region of the body.

Production of High Permittivity Pads

High permittivity pads were produced based on the approach described previously.[19] Briefly, barium titanate ($BaTiO^3$) powder (Alfa Aesar GmbH) was mixed with water until a saturated suspension was reached since the aim was to produce as high a permittivity as possible. Approximately, a 4:1 weight/weight ratio of barium titanate powder to water was used. The dielectric constant was measured using a dielectric probe kit (85070E, Agilent Technologies, Santa Clara, CA) and a network analyzer, and had a value of 300. This is substantially higher than reported in a previous publication,[19] and emphasizes the fact that the permittivity that can be reached is critically dependent upon the surface properties and size of the barium titanate powder used. Two pads, each 1 cm thick, of the suspension were heat-sealed within polypropylene pads, with dimensions 28 x 22 cm^2 (left/right and head/foot dimensions, respectively). The weight of these pads was approximately 2 kg, significantly less both in thickness and weight compared to a commercial water-based pad (3 cm thick and 3.2 kg weight).

MRI Protocols

All experiments were approved by the Leiden University Medical Center Committee for Medical Ethics, and performed on a dual-transmit 3 T Philips Achieva. Nine volunteers (seven male, two female), with ages between 25 and 50, and body mass indices (BMIs) between 18 and 38, were imaged. The transmit coil was the inbuilt body resonator, and a six-element ''cardiac array'' was used for signal reception: this consisted of three elements anterior and three elements posterior to the patient. All experiments were performed first with the pads in place, the pads were then removed with as little subject motion as possible, and rescanning without the pads was performed. Figure 1 shows a schematic of the EM simulation setup accompanied by a photograph of the positioning of the thin pad on the anterior side of the volunteer. The transmit field of the body coil was mapped using the method of Yarnykh at 2.5 mm isotropic resolution with a target angle of 45° to avoid ambiguity for any actual tip angle close to or greater than 90°.[21] Imaging parameters: three-dimensional gradient echo sequence: echo time = 20 ms, TR1 = 100 ms, TR2 = 250 ms, nominal flip angle 50°, 64 x 64 data matrix, transverse slice thickness 10 mm, 1 mm slice gap, field-of-view ~ 250 x 450 x 120 mm^3 with slight variations dependent upon subject size. Tip angle maps were generated from the ratio of the signal intensities obtained with the two different pulse repetition time values. Tip angle maps were then converted to transmit sensitivity (B_1^+ per square root of power) for direct comparison with EM simulations. Coefficient of variation values were calculated as described in the previous section. For assessment of image quality, T^1-weighted turbo gradient echo sequences were run with the following parameters: echo time = 2.3 ms, pulse repetition time = 10 ms, tip angle = 15°, 252 x 149 data matrix, slice thickness = 7 mm, 1 mm slice gap, field-of-view = 297 x 375 x 77 mm^3, acquisition time = 13.5 s for six slices, linear phase encoding, scan percentage 75%, turbo echo factor 149, no flow compensation. Images were acquired during breathhold (exhalation).

Four different settings were used to investigate the separate effects of RF shimming and the dielectric pads. First, RF shimming was turned off forcing the conventional quadrature relationship between the two separate transmit channels. Second, RF shimming was enabled, in which a rapid grid search is performed by the Philips system with a free range of relative amplitudes and phase difference between the two channels. RF shimming was performed separately for the cases with and without the dielectric pads in place.

Measurements of the time-averaged power during the imaging sequence are recorded in the log file of the scanner. These measurements are performed directly at the amplifier, and measure both the forward and reflected powers, the difference between the two being the power delivered to the system (losses in cables and connectors between the RF amplifiers and the RF coil may be up to 15%, but this percentage does not vary significantly with absolute power).

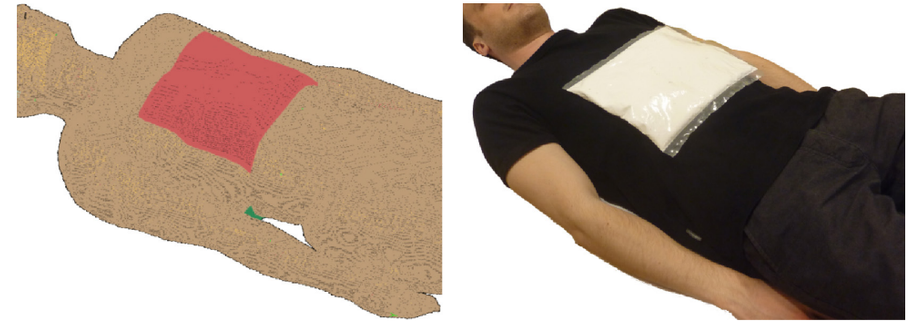

FIGURE 1. (left) Schematic of the setup for the EM simulations with a dielectric pad (red) with thickness 1 cm placed on the abdomen. An identically shaped pad (green) is placed on the back, in the same position. (right) photograph of a volunteer with the pads in place. [Color figure can be viewed in the online issue, which is available at wileyonlinelibrary.com.]

Statistical Analysis

Statistical analysis was performed using Graphpad Prism (La Jolla, CA). Paired two-sided Student's t-tests were performed for conditions of with/without dielectric pads for data acquired with and without the dielectric pads.

RESULTS

EM Simulations

Figure 2 shows simulation results of the B_1^+ field in the male Duke model. The grid search gave an optimum configuration with relative permittivities of 400 for the anterior pad and 500 for the posterior pad for a pad thickness of 1 cm. In practice, the highest permittivity that could be achieved was 300 using essentially a saturated suspension of barium titanate powder in water.

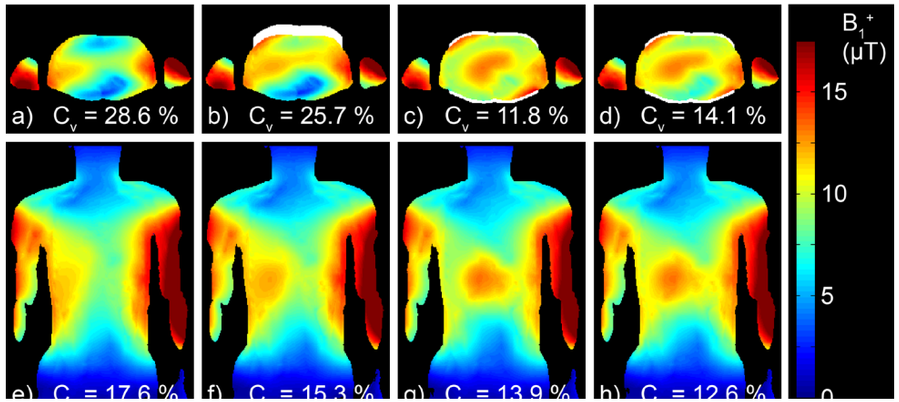

FIGURE 2. EM simulations of the B_1^+ field in the "Duke" model. (a)–(d) transverse slice through the centre of the liver, (e)–(h) corresponding coronal slices. (a) and (e) no dielectric pads, (b) and (f) a 3 cm thick "commercial" water-based pad, (c) and (g) the optimum solution for two 1 cm thick pads with ε_r = 400 for the anterior pad and ε_r = 500 for the posterior pad, (d) and (h) the practically realizable situation with two 1 cm pads each with ε_r = 300. The coefficient of variation is shown for each configuration.

In Figure 2, the values of C_v are given for the situations of no pads, the commercial pad (3 cm thick, water-based, ε_r = 80), the optimum configuration of the two pads placed anterior and posterior, and the practical configuration of two pads with relative permittivities of 300. As outlined in the methods section, in the transverse slice, the value of C_v is calculated throughout the entire cross-section (not considering the arms), and for the coronal slice through the thorax and abdominal region of the body. There are considerable improvements in the B_1^+ homogeneity for the anterior/posterior high permittivity pads compared to both the situation with no pads, and also the asymmetric placement of the commercial pad on only the anterior side of the subject. It should be noted that, since optimization was performed on the transverse slice due to the much more defined region-of-interest (essentially the entire slice without the arms), the value of C_v in the coronal plane can actually be slightly lower for the ε_r = 300 case than the "optimum" permittivity value.

Figure 3 shows corresponding plots for the female Ella model. In this case, the optimum configuration was found to correspond to relative permittivities of 300 for the front and back. The dependence of the value of C_v on the permittivities of the two pads for both the Duke and Ella model is shown in Figure 4. As can be seen, there is a relatively smooth minimum for values around 300 – 500, but the increase is quite severe for values below about 300 or above 500. These results confirm the simulation results in Figure 2 which demonstrate that there is a very small increase in C_v when operating with pads with permittivity of 300 compared to the optimum values of 400/500.

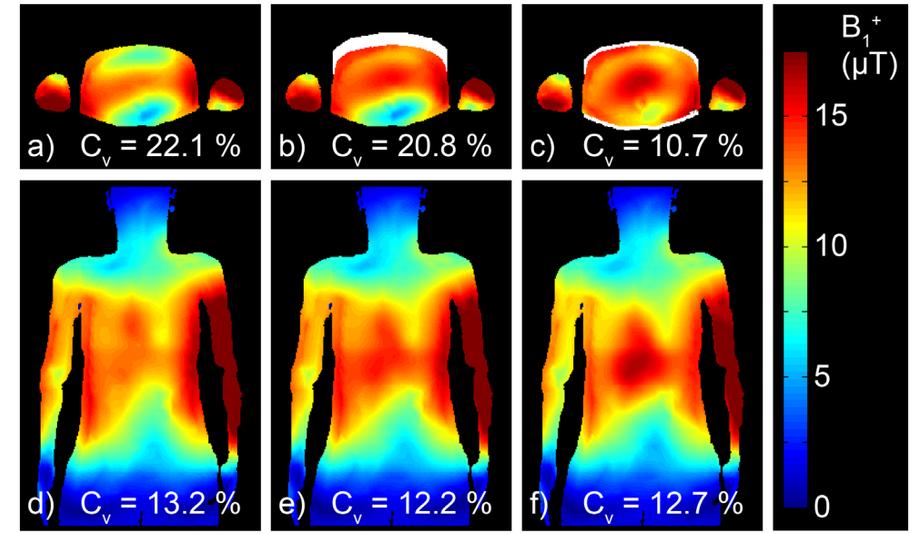

FIGURE 3. EM simulations of the B_1^+ field in the "Ella" model. (a)–(c) transverse slice through the centre of the liver, (d)–(f) corresponding coronal slices. (a) and (d) no dielectric pads, (b) and (e) a 3 cm thick "commercial" water-based pad, (c) and (f) the optimum solution for two 1 cm thick pads each with ε_r = 300. The coefficient of variation is shown for each configuration.

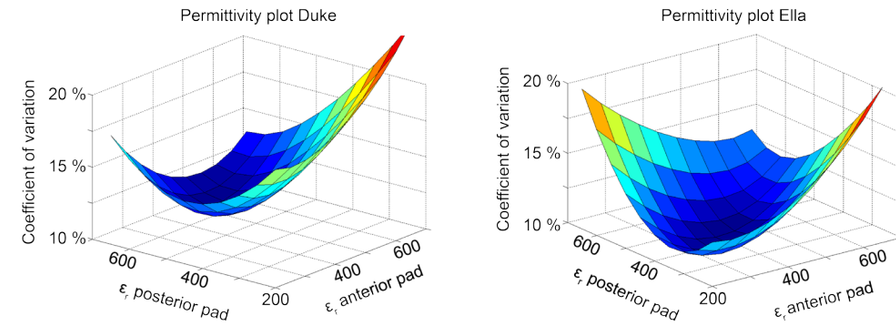

FIGURE 4. Plots of the coefficient of variation (vertical axis) versus the permittivities of both the anterior and posterior pads. (left) Duke and (right) Ella models.

[Color figure can be viewed in the online issue, which is available at wileyonlinelibrary.com.]

To determine whether the high permittivity pads increase either the local or global SAR values, Figure 5 shows transverse and coronal plots of the local (1 g tissue average) SAR values for the Duke model generated by the quadrature-driven body coil. The highest values are generally found in the arms (since they are in the region of the highest electric field of the RF coil), and all values in the body are at least a factor-of-two lower. There are negligible differences introduced by either the commercial or new high permittivity pads. Very similar results were found for Ella (data not shown). These results correspond to the conventional quadrature-driven body coil, but it is anticipated that similar effects occur in the RF-shimmed case.

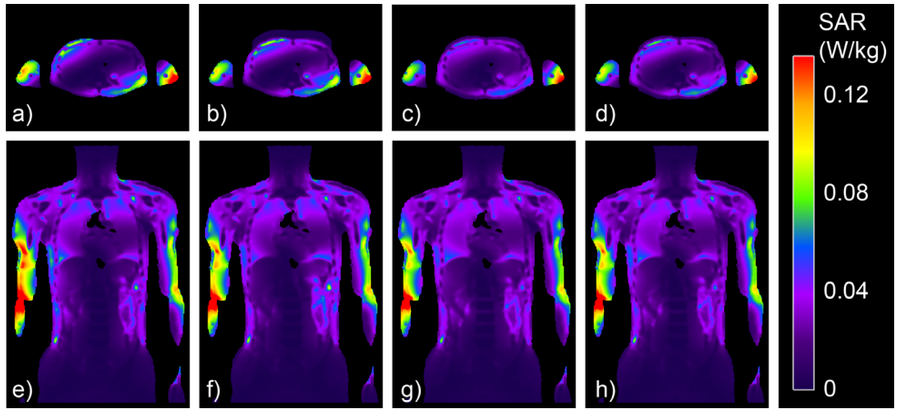

FIGURE 5. EM simulations of the 1-g averaged SAR in the ''Duke'' model. a–d: transverse slice through the centre of the liver, (e)–(h) corresponding coronal slices. (a) and (e) no dielectric pads, (b) and (f) a 3 cm thick ''commercial'' water-based pad, (c) and (g) the optimum solution for two 1 cm thick pads with $\varepsilon_r = 400$ for the anterior pad and $\varepsilon_r = 500$ for the posterior pad, (d) and (h) the practically realizable situation with two 1 cm pads each with $\varepsilon_r = 300$. [Color figure can be viewed in the online issue, which is available at wileyonlinelibrary.com.]

Experimental Results

Figure 6 shows transverse slices acquired for five of the nine volunteers (for clarity) for all four configurations of with/without RF shimming and with/without high permittivity pads. Clear improvements in image homogeneity are evident with the addition of the pads.

Figure 7 demonstrated the B_1^+ maps acquired without and with the dielectric pads in place for the same volunteers and the same conditions as shown in Figure 6. There is good agreement with the simulated results presented in Figure 2.

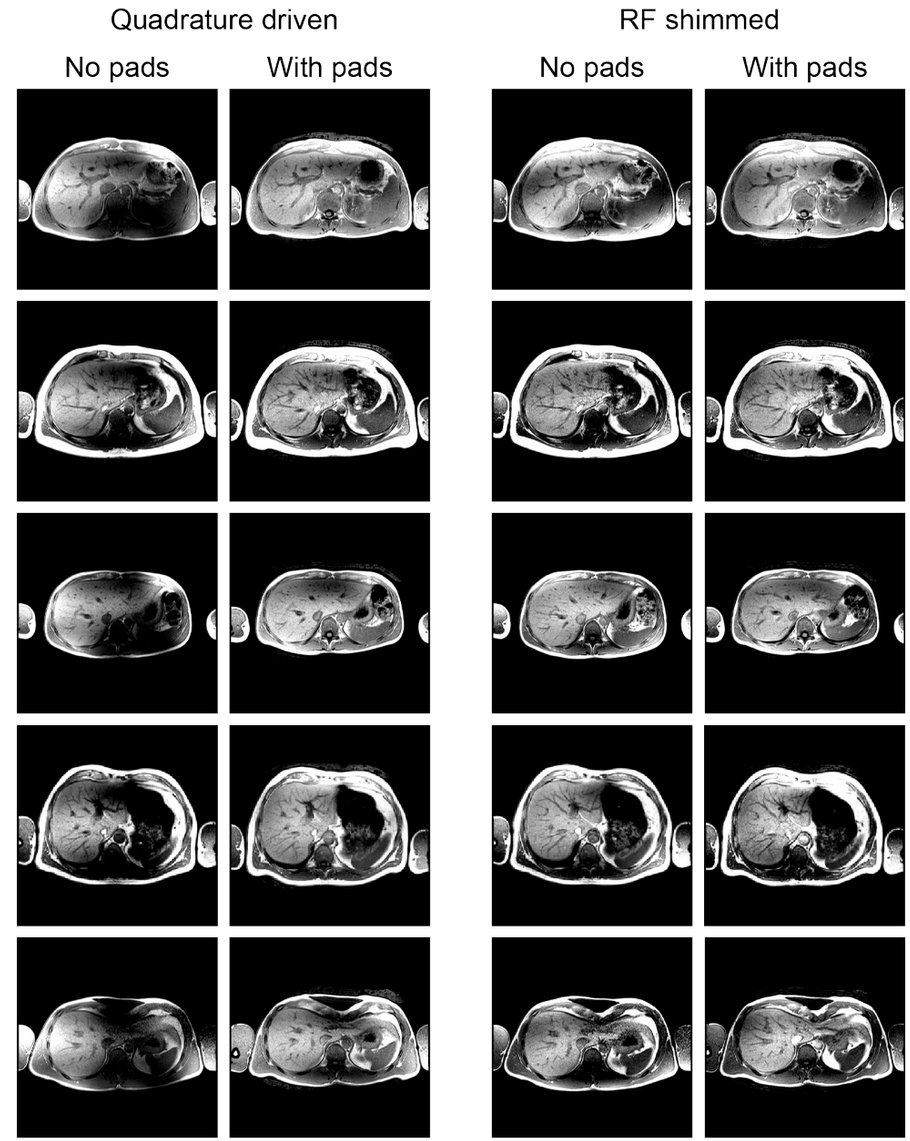

FIGURE 6. Comparison of T^1-weighted turbo-spin echo images acquired from five volunteers with BMI values between 18 and 24 for four different configurations of quadrature/RF-shimmed drive and without/with dielectric pads.

Figure 8 shows a plot of the C_v for all nine volunteers for the four different imaging conditions. For the quadrature drive, the C_v decreased in all cases, and often by a substantial amount (mean 25.4 ± 10%), with the addition of the dielectric pads. In the RF shimmed case, a decrease (mean 16 ± 13%) in C_v for all but one case was achieved using the pads. Statistical analysis showed a significant decrease ($P < 0.0001$) in C_v between quadrature mode without and with the dielectric pads, and also in the RF shimmed case without and with the pads ($P = 0.005$).

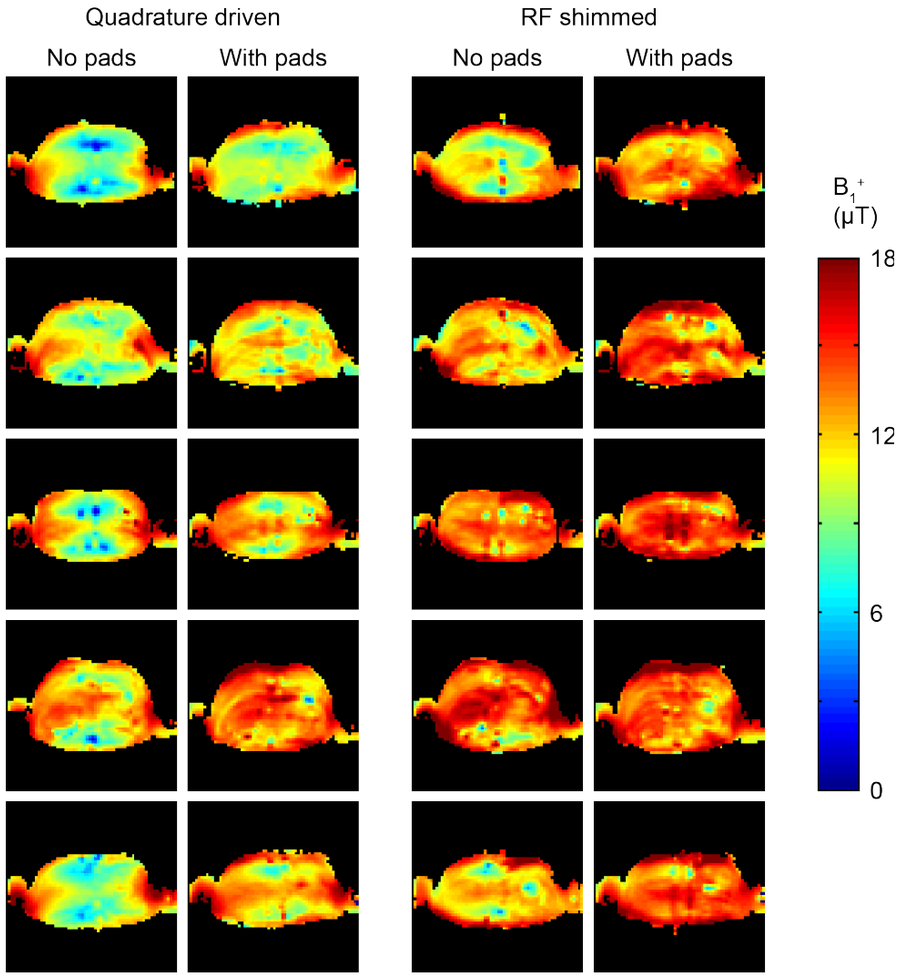

FIGURE 7. Measured B^{1+} maps from the same volunteers as in Fig. 6 for the same four configurations. [Color figure can be viewed in the online issue, which is available at wileyonlinelibrary.com.]

In terms of the RF power required for image acquisition, there were also statistically significant reductions in both the peak power and time-averaged power using the dielectric pads. As with most power optimization algorithms on commercial systems, the average flip angle across the central transverse slice is calibrated. In the case of an inhomogeneous B_1^+ distribution, this causes overtipping in areas of high transmit efficiency, and undertipping in areas of low efficiency.

Figure 9 shows the time-averaged power needed for the T1-weighted turbo gradient echo sequence used to produce the images in Figure 6: these powers were read from the log file that was stored on the scanner, with the powers being measured at the output of the RF amplifier as described in the methods section. The power demands were in all but one case lower with pads than without pads. Statistical analysis showed a significant decrease in average power when the high permittivity pads were in place for both the quadrature-driven mode ($P = 0.01$) and RF shimmed mode ($P = 0.0004$).

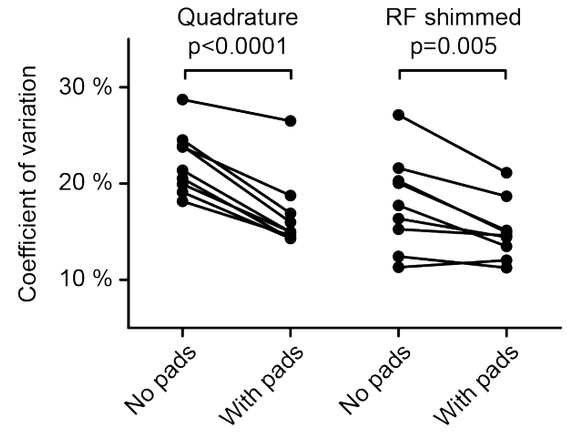

FIGURE 8. Plot of coefficient of variation for all nine volunteers. Statistically significant decreases are shown for both quadrature driven and RF-shimmed cases when introducing the dielectric pads.

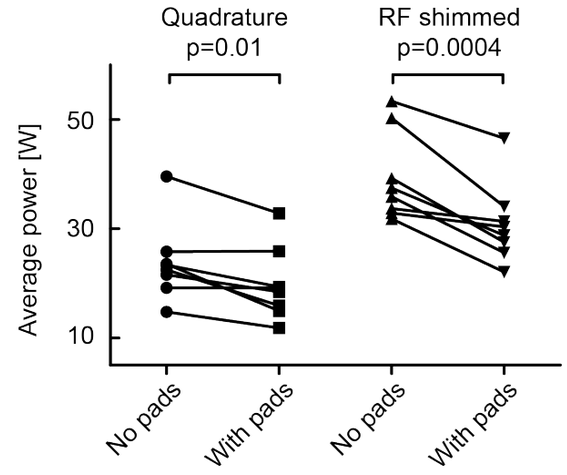

FIGURE 9. Plot of time averaged power measured for the images acquired in Fig. 6 for all nine volunteers. Statistically significant decreases are shown for both quadrature-driven and RF-shimmed cases when introducing the dielectric pads.

DISCUSSION AND CONCLUSION

The intrinsic inhomogeneity introduced by imaging an elliptical object with a quadrature RF coil is well known,[22] and different patient geometries may mitigate or exacerbate this effect. The recent commercial introduction of dual-transmit systems has shown substantial improvement in image quality, but does not yet represent a complete solution to the problem. The ''ability'' of high permittivity materials [23] to increase the homogeneity of the transmit magnetic field has been shown primarily for neuroimaging at high field either with water bags [24] or materials formed from metal titanates.[18,19,25] Recently, improvements for neuroimaging at 3 T have also been reported using large water pads.[26] The lower the magnetic field, the higher the permittivity must be to compensate for B_1 inhomogeneities since displacement currents are proportional to the operating frequency. In neuroimaging at 7 T, the optimum value of the permittivity was found to be 100.[20] In this current work, we have demonstrated that statistically significant improvements in transmit efficiency for abdominal imaging at 3 T can be achieved using thin, high permittivity pads placed anterior and posterior to the subject. There are large measured improvements when operating the system in quadrature mode, which corresponds to the vast majority of single channel 3 T systems currently available in the world. Even when operating in dual transmit mode with RF shimming on a state-of-the-art multichannel system, the dielectric pads provided a statistically significant increases in image homogeneity, as well as a reduction in the total power absorbed by the body.

The geometry which we studied is relatively simple, consisting only of two pads of 1 cm thickness, and certainly it can be anticipated that further improvements may result from optimized geometries including more pads in a more complex geometry. Another refinement would be to optimize the coefficient of variance over the entire three-dimensional imaging volume, rather than just a central slice as in this work. Higher permittivity materials should bring further increases in image quality, as well as reduction in the thickness of the required pads, particularly in the case of patients with higher body mass index values than in healthy volunteers studied here. The current study does not have enough volunteers, or volunteers with sufficient range of BMI values, to be able to relate directly the improvements afforded by the dielectric pads to the BMI, or probably even more relevant to the geometry of the body. Future clinical studies including patients with much higher BMI will be required to establish such a relationship. In this work no increases in global SAR (assuming body loss dominance) were evident, and indeed a reduction in local SAR was simulated for the quadrature-driven body coil. This was experimentally demonstrated by measuring substantial reductions in average power levels on the MR system both for the quadrature-driven mode, and also the RF shimmed mode.

ACKNOWLEDGMENTS

The authors are grateful to Sukhoon Oh and Chris Collins at the Hershey Medical Center for providing the body coil model, and to Wouter Teeuwisse for helping in data acquisition.

REFERENCES

1. Bernstein MA, Huston J, III, Ward HA. Imaging artifacts at 3.0T. J Magn Reson Imaging 2006;24:735–746.

2. Cornfeld D, Weinreb J. Simple changes to 1.5-T MRI abdomen and pelvis protocols to optimize results at 3 T. Am J Roentgenol 2008; 190:W140–W150.

3. Chang KJ, Kamel IR. Abdominal imaging at 3T: challenges and solutions. Appl Radiol 2010;39:22–31.

4. Dietrich O, Reiser MF, Schoenberg SO. Artifacts in 3-T MRI: Physical background and reduction strategies. Eur J Radiol 2008;65:29–35.

5. Yang RK, Roth CG, Ward RJ, deJesus JO, Mitchell DG. Optimizing abdominal MR imaging: approaches to common problems. Radiographics 2010;30:185–199.

6. Merkle EM, Dale BM. Abdominal MRI at 3.0 T: the basics revisited. Am J Roentgenol 2006;186:1524–1532.

7. Nelles M, Konig RS, Gieseke J, Guerand-van Battum MM, Kukuk GM, Schild HH, Willinek WA. Dual-source parallel RF transmission for clinical MR imaging of the spine at 3.0 T: intraindividual comparison with conventional single-source transmission. Radiology 2010; 257:743–753.

8. Willinek WA, Gieseke J, Kukuk GM, Nelles M, Konig R, Morakkabati- Spitz N, Traber F, Thomas D, Kuhl CK, Schild HH. Dual-source parallel radiofrequency excitation body MR imaging compared with standard MR imaging at 3.0 T: initial clinical experience. Radiology 2010;256:966–975.

9. Adriany G, van de Moortele PF, Wiesinger F, et al. Transmit and receive transmission line arrays for 7 Tesla parallel imaging. Magn Reson Med 2005;53:434–445.

10. Vaughan JT, Snyder CJ, DelaBarre LJ, Bolan PJ, Tian J, Bolinger L, Adriany G, Andersen P, Strupp J, Ugurbil K. Whole-body imaging at 7T: preliminary results. Magn Reson Med 2009;61:244–248.

11. Kraff O, Bitz AK, Kruszona S, Orzada S, Schaefer LC, Theysohn JM, Maderwald S, Ladd ME, Quick HH. An eight-channel phased array RF coil for spine MR imaging at 7 T. Invest Radiol 2009;44:734–740.

12. van den Berg CA, van den Bergen B, Van de Kamer JB, Raaymakers BW, Kroeze H, Bartels LW, Lagendijk JJ. Simultaneous B1 þ homogenization and specific absorption rate hotspot suppression using a magnetic resonance phased array transmit coil. Magn Reson Med 2007;57:577–586.

13. Vernickel P, Roschmann P, Findeklee C, Ludeke KM, Leussler C, Overweg J, Katscher U, Grasslin I, Schunemann K. Eight-channel transmit/ receive body MRI coil at 3T. Magn Reson Med 2007;58:381–389.

14. Franklin KM, Dale BM, Merkle EM. Improvement in B1-inhomogeneity artifacts in the abdomen at 3T MR imaging using a radiofrequency cushion. J Magn Reson Imaging 2008;27:1443–1447.

15. Sreenivas A, Lowry M, Gibbs P, Pickles M, Turnbull LW. A simple solution for reducing artefacts due to conductive and dielectric effects in clinical magnetic resonance imaging at 3 T. Eur J Radiol 2007;62:143–146.

16. Takayama Y, Nonaka H, Nakajima M, Obata T, Ikehira H. Reduction of a high-field dielectric artifact with homemade gel. Magn Reson Med Sci 2008;7:37–41.

17. Kataoka M, Isoda H, Maetani Y, et al. MR imaging of the female pelvis at 3 Tesla: evaluation of image homogeneity using different dielectric pads. J Magn Reson Imaging 2007;26:1572–1577.

18. Teeuwisse WM, Brink WM, Webb AG. Quantitative assessment of the effects of high-permittivity pads in 7 Tesla MRI of the brain. Magn Reson Med 2012;67:1285–1293.

19. Teeuwisse WM, Brink WM, Haines K, Webb AG. Simulations of high permittivity materials for 7 T neuroimaging and evaluation of a new barium titanate-based dielectric. Magn Reson Med 2012;67: 912–918.

20. Christ A, Kainz W, Hahn EG, et al. The Virtual Family-development of surface-based anatomical models of two adults and two children for dosimetric simulations. Phys Med Biol 2010;55:N23–N38.

21. Yarnykh VL. Actual flip-angle imaging in the pulsed steady state: A method for rapid three-dimensional mapping of the transmitted radiofrequency field. Magn Reson Med 2007;57:192–200.

22. Sled JG, Pike GB. Standing-wave and RF penetration artifacts caused by elliptic geometry: an electrodynamic analysis of MRI. IEEE Trans Med Imaging 1998;17:653–662.

23. Webb AG. Dielectric materials in magnetic resonance. Concepts Magn Reson 2011;38A:48–84.

24. Yang QX, Mao W, Wang J, Smith MB, Lei H, Zhang X, Ugurbil K, Chen W. Manipulation of image intensity distribution at 7.0 T: passive RF shimming and focusing with dielectric materials. J Magn Reson Imaging 2006;24:197–202.

25. Snaar JE, Teeuwisse WM, Versluis MJ, van Buchem MA, Kan HE, Smith NB, Webb AG. Improvements in high-field localized MRS of the medial temporal lobe in humans using new deformable highdielectric materials. NMR Biomed 2011;24:873–879.

26. Yang QX, Wang JL, Wang JH, Collins CM, Wang CS, Smith MB. Reducing SAR and Enhancing Cerebral Signal-to-Noise Ratio with High Permittivity Padding at 3 T. Magn Reson Med 2011;65:358–362.